Arabian Journal of Geosciences (2022) 15: 446
https://doi.org/10.1007/s12517-022-09724-w

ORIGINAL PAPER

Hydro-thermal characteristics and deformation behaviors of silty clay subjected to freeze–thaw cycles

Jianguo Lu[1,2] · Xusheng Wan[1] · Zhongrui Yan[1] · Nima Pirhadi[1] · Xiaoyi Fan[1] · Mingnan Sun[3]

Received: 13 September 2021 / Accepted: 16 February 2022 / Published online: 1 March 2022

Abstract

In cold regions, hydro-thermal characteristics and deformation behaviors of soils are important factors to evaluate the stabilities of engineering. In this study, the volumetric unfrozen water contents and deformations of silty clay exposed to freeze–thaw cycles were experimentally investigated, as well as dry density and porosity. The results showed that, in the first fifteen freeze–thaw cycles, the volumetric unfrozen water content, deformation, dry density, and porosity greatly changed. Besides, the influence of water seepage on volumetric unfrozen water content of soils is larger than that of the water migration during freeze–thaw cycles, the residual volumetric unfrozen water contents of soils are mainly determined by the lowest ambient temperature. Furthermore, the freeze–thaw actions make opposite effects on the soils with different dry densities, namely, the dense soils with high densities are expanded, while the soils with low densities are compressed after freeze–thaw cycles. There is a critical dry density and residual porosity where the soil samples does not change its volumes, dry densities, and porosities. For the silty clay, the critical dry density is around 1.60 g/cm^3, and the residual porosity ranges from 0.40 to 0.41.

Keywords Freeze–thaw cycles · Volumetric unfrozen water content · Deformation · Dry density · Porosity

Introduction

Freeze–thaw cycles, as weathering processes, have significant effects on the performance of earthwork structures, such as railway and highway embankments (Ma et al. 2019; Wu and Niu 2012), tunnel (Li et al. 2017a; Zhang et al. 2017a), dam embankments (Zhang et al. 2021), foundation (Liu et al. 2015), and canal (Li et al. 2014, 2015). In cold regions, engineering structures are subjected to at least one freezing and thawing process every year (Kalkan 2009); for the soils near the surface layer, the number of freeze–thaw cycles might be more than one time due to the fluctuations of air temperatures (Aldaood et al. 2016; Hohmann-Porebska 2002). It has been found that the physical characteristics of soils are changed after cyclic freeze–thaw, such as unfrozen water content (Kozlowski and Nartowska 2013; Tian et al. 2019), matric suction (Lu et al. 2019), thermal conductivity (Zhang et al. 2018a), deformation (Lu et al. 2018), free energy (Yao et al. 2009), permeability (Chamberlain and Gow 1979; Viklander and Eigenbrod 2000), microstructure (Aldaood et al. 2016; Tian et al. 2019), grain-size distribution (Moghbel and Fall, 2016), shear strength (Cui et al. 2014; Liu et al. 2019a, b), and damping ratio (Zhao et al. 2020). Their changes are related to many factors, e.g., soil types, depth of frost heave, number of freeze–thaw actions, and duration of freezing and thawing processes (Kamei et al. 2012; Simonsen et al. 2002). Therefore, to accurately select soil parameters for deformation analysis and stability evaluation of engineering, e.g., embankments, tunnels, slopes, and airports in cold regions, especially those underlain by deep seasonally frozen areas and permafrost, the variation of soil properties due to the effect of freeze–thaw actions must be taken into account.

Some studies have been conducted to study the variations of mechanical and physical properties of soils subjected

Communicated by Zeynal Abiddin Erguler.

✉ Xusheng Wan
xinyanwanxxusheng@163.com

[1] School of Civil Engineering and Geomatics, Southwest Petroleum University, Chengdu 610513, China

[2] State Key Laboratory of Frozen Soil Engineering, Northwest Institute of Eco-Environment and Resources, Chinese Academy of Sciences, Lanzhou 730000, China

[3] Institute of Safety, Environment Protection and Technical Supervision, PetroChina Southwest Oil & Gas Field Company, Chengdu 610041, China

to freeze–thaw actions. Liu et al. (2019a) investigated the variations of the volume of unsaturated silty clays during freezing processes and found that there is a critical saturation degree. For a given soil sample, when the initial saturation degree is lower than the critical saturation degree, frost shrink happens. Otherwise, the frost heave and frost crack occur. Qi et al. (2008) overall concluded the variations of the mechanical properties and physical characteristics for the soils after the freeze–thaw actions, e.g., hydraulic permeability, void ratio and density, Atterberg limits, resilient modulus, undrained shear strength, etc. This study gives us significant guidance to better understand the freeze–thaw actions on properties of soils. Li et al. (2017b) studied the freeze–thaw cycles on properties of compacted loess, and obtained that the density of the upper soil layers significantly changed due to freeze–thaw erosions. These results imply that many properties of soils are significantly varied after freeze–thaw actions, especially for the mechanical and physical properties. However, for the above studies, the duration of freeze–thaw actions was quite limited. Therefore, the soil samples could hardly retain a balanced structure. Consequently, to some extent, the representative values, such as critical dry density, residual porosity, and their corresponding number of freeze–thaw cycles, could not be obtained.

In cold regions, hydro-thermal characteristics and deformation behaviors of soils are significant factors in determining the stabilities and assessing the risks of engineering, especially in permafrost. When soils are exposed to freezing process, and the soil temperature is in the negative temperature, the water–ice phase transition occurs. Consequently, the frost heave might subsequently happen. Otherwise, during the thawing process, the thaw settlement would occur. Generally, some hydro-thermal phenomenon (e.g., heat transfer, moisture migration, water redistribution, ice formation and accumulation) and deformation characteristics (e.g., frost heave, thaw settlement, cold shrink, and thermal bulge) are accompanied with freezing and thawing processes (Qi et al. 2006, 2008; Lu et al. 2018; Zhang et al. 2017b), and these hydro-thermal and deformation phenomena are basic factors in determining the stability and assessing the risks of engineering in cold regions. Furthermore, if the soils are exposed to freeze–thaw actions, then the hydro-thermal characteristics and deformation behaviors are more complicated. In the study of hydro-thermal characteristics, many studies have been carried out to investigate the variations of thermal properties (Lu et al. 2021), water migration and redistribution (Tian et al. 2018; Wan et al. 2019; Zhang et al. 2018b), ice formation and salt crystallization of soils (Lai et al. 2017; Wan et al. 2017). In terms of deformation behaviors, it is found that the freeze–thaw cycles have significant influences on the characteristic variable deformation due to the changes of pore distribution and structure of soils during the first freeze–thaw cycle (Lu et al. 2018). Besides, some other studies are focused on the frost heave and thaw settlement behaviors of soils after freeze–thaw actions (Lai et al. 2017; Zhang et al. 2017c).

It can be seen that much works have been carried out to study the variations of the mechanical and physical characteristics of soils exposed to freeze–thaw actions. However, there are barely studies focusing on the hydro-thermal characteristics and deformation behaviors of soils during freeze–thaw cycles. Therefore, in this study, some laboratory experiments were performed to investigate the hydro-thermal characteristics and deformation behaviors, as well as variations of the dry density and porosity of soils subjected to freeze–thaw cycles.

Experimental design

Experimental apparatus

Figure 1 shows the freeze–thaw apparatus used in this experiment, and it consists of three systems, namely, insulation chamber, temperature-controlled unit, and data acquisition unit. The insulation chamber is surrounded with a 5-cm-thick insulation rigid polyurethane board, and the insulation chamber dimension is 50 cm (length) × 50 cm (width) × 55 cm (height). The temperature-controlled unit includes an air cooler, three cooling fans, an auto temperature controller, and an inner chamber temperature sensor. The temperature of the insulation chamber is controlled by the three cooling fans installed at the top and sides of the chamber, and the three cooling fans are connected to the air cooler, which generates cooling or heating. Eventually, the insulation chamber is controlled in a desired temperature after the auto temperature

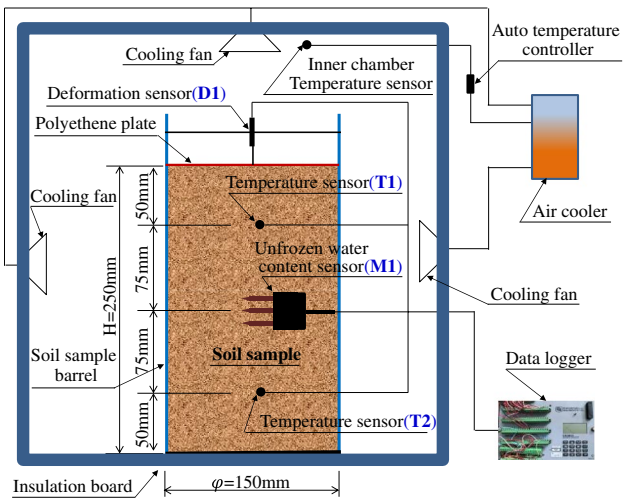

Fig. 1 Schematic of experimental equipment

controller is automatically set according to the feedback values of the inner chamber temperature sensor (Fig. 1).

The data acquisition unit included deformation sensor, unfrozen water content sensor, and temperature sensors (Fig. 1). The deformation sensor (linear displacement sensors) with a precision of ± 0.1 F.S. (full scale) is arranged on the top of the soil samples (D1). The unfrozen water content sensor (dielectric permittivity soil moisture sensor) with a precision of ± 0.03 m^3/m^3 and a working temperature ranging from − 40 to + 50 °C was located at the middle of the soil sample (M1) (sensor calibration as shown below). The temperature sensors (thermistors) with a temperature range of − 30 to + 30 °C and a precision of ± 0.05 °C were buried at the depth of 5 cm from the top (T1) and depth of 5 cm from the bottom (T2), respectively. Eventually, a data logger was used to connect the sensors, and the data are automatically collected every 5 min (Fig. 1).

Sensor calibration

To accurately measure the unfrozen water contents, it is essential to calibrate the unfrozen water content sensors using the silty clay. For a given soil, the dielectric permittivity soil moisture sensors are relevant to the volume of liquid water and the volume of soils, the gravimetric water content was changed to volumetric unfrozen water content as follows:

$$\theta_u = \frac{w\rho_d}{\rho_w} \tag{1}$$

where θ_u and w are volumetric and gravimetric unfrozen water contents of soils, respectively. ρ_d and ρ_w are dry density of soil and water density, respectively. Based on the Topp et al. (1980) and the Eller and Denoth (1996) equations, a third-order polynomial equation was used to calculate the volumetric unfrozen water contents:

$$\theta_u = aK_a^3 + bK_a^2 + cK_a + d \tag{2}$$

where a, b, c, and d are fitting parameters; K_a is the dielectric permittivity of soils, and the fitting parameters are summarized in Table 1, it presents the correlation coefficient for the fitting equation in this study ($R^2 = 0.9958$), which is nearly 1, indicating the strong positive correlation for the silty clay (Table 1).

The calibration curve of volumetric unfrozen water content is presented in Fig. 2. It shows that, in the range with low water contents, the measured volumetric unfrozen water contents have good agreement with the calculated ones by the Topp et al. (1980) equation, while in the range with large water contents, the volumetric unfrozen water contents calculated by the Topp et al. (1980) equation are larger than the measured ones, and it indicates that in this range the Topp et al. (1980) equation might overestimate the volumetric unfrozen water contents of silty clay.

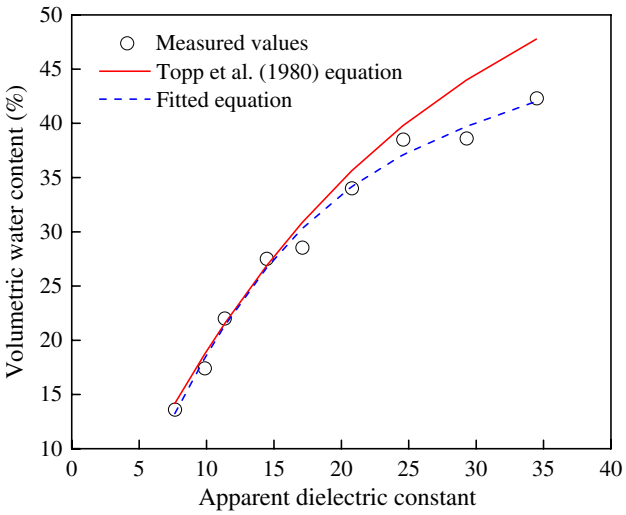

Fig. 2 Calibration curve of unfrozen water content

Experimental procedure

The silty clay comes from the soils widely distributed in the Hexi Corridor on the northwest of China. The particle size distribution of the soil is shown in Fig. 3, and its liquid and plastic limits are 29.81% and 18.54%, respectively. Besides, the thermal conductivities of the soil in frozen and unfrozen states are 1.83 W/(m.℃) and 1.19 W/(m.℃), respectively. Here, six column soil samples were prepared, the heights of the soil samples are 25.0 cm, and the diameters are 15.0 cm (Table 1 and Fig. 1). Besides, the initial gravimetric water contents of soil samples are all 17.4% (Table 2). In order to investigate the water migration and water seepage under the action of freeze–thaw cycles, the volumetric unfrozen water contents in soil sample No. VI (Table 2) at the positions of 50 mm and 125 mm from the top were measured and analyzed.

Besides, in order to study the ambient temperature on the hydro-thermal characteristics and deformation behaviors of silty clay, two ambient controlled temperature conditions were performed, the highest ambient temperatures for the

Table 1 Parameters of regression equations

Types of equation	a	b	c	d	R^2
Topp et al. (1980) equation	4.30×10^{-6}	-5.50×10^{-4}	2.92×10^{-2}	-5.30×10^{-2}	0.9791
Fitted equation in this study	8.07×10^{-6}	-8.57×10^{-4}	3.46×10^{-2}	-8.36×10^{-2}	0.9958

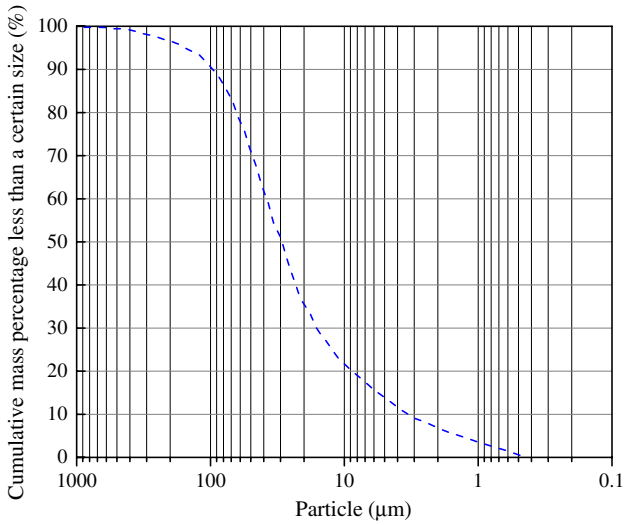

Fig. 3 Particle size distribution

two controlled ambient temperature conditions are + 9.0 °C, and the lowest ambient temperatures for the controlled ambient temperature conditions 1 and 2 are − 8.0 °C and − 3.0 °C, respectively (Table 2 and Fig. 4). Before the experiment, the soil sample were set for 12 h under an ambient temperature of + 9.0 °C to reach a hydro-thermal equilibrium state. Then, the ambient temperatures were decreased gradually from + 9.0 to − 8.0 °C and − 3.0 °C for the controlled ambient temperature conditions 1 and 2, respectively (Fig. 4). Subsequently, during the warming processes, the ambient temperatures were gradually increased from − 8.0 and − 3.0 to + 9.0 °C for the controlled ambient temperature conditions 1 and 2, respectively (Fig. 4). For the soil samples, a total of 39 freeze–thaw cycles were applied in the experiment (Fig. 4).

Results and analysis

Analysis of hydro-thermal characteristics

Figures 5 and 6 present the volumetric unfrozen water contents for the controlled ambient temperature conditions 1 and 2 under the action of freeze–thaw cycles, respectively. The figures show that the change of maximum volumetric unfrozen water contents for the six soil samples in freeze–thaw cycles could be distinguished into two stages, namely, increasing stage and stable stage (Figs. 5 and 6). In detail, for the increasing stage, the maximum volumetric unfrozen water contents gradually increase from the first to the fifteen freeze–thaw cycles. For the stable stage, the maximum

Table 2 Design of soil samples

Sample no	Initial dry density (g/cm^3)	Initial gravimetric water content (%)	Porosity	Column size (h (mm) × φ (mm))	Controlled ambient temperature (°C)	
					Lowest	Highest
I	1.45	17.40	0.4630	250 × 150	− 8.00	+ 9.00
II	1.55	17.40	0.4260	250 × 150	− 8.00	+ 9.00
III	1.60	17.40	0.4074	250 × 150	− 8.00	+ 9.00
IV	1.60	17.40	0.4074	250 × 150	− 3.00	+ 9.00
V	1.62	17.40	0.4000	250 × 150	− 3.00	+ 9.00
VI	1.70	17.40	0.3704	250 × 150	− 3.00	+ 9.00

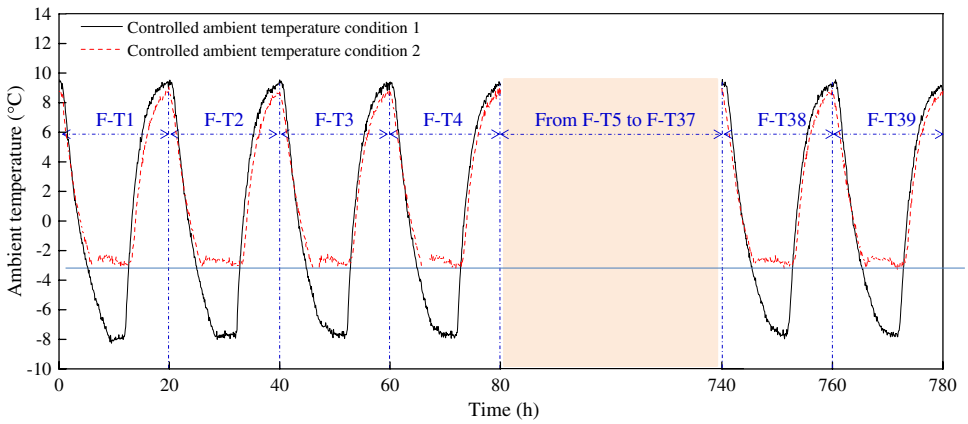

Fig. 4 Monitored ambient temperatures in experiments

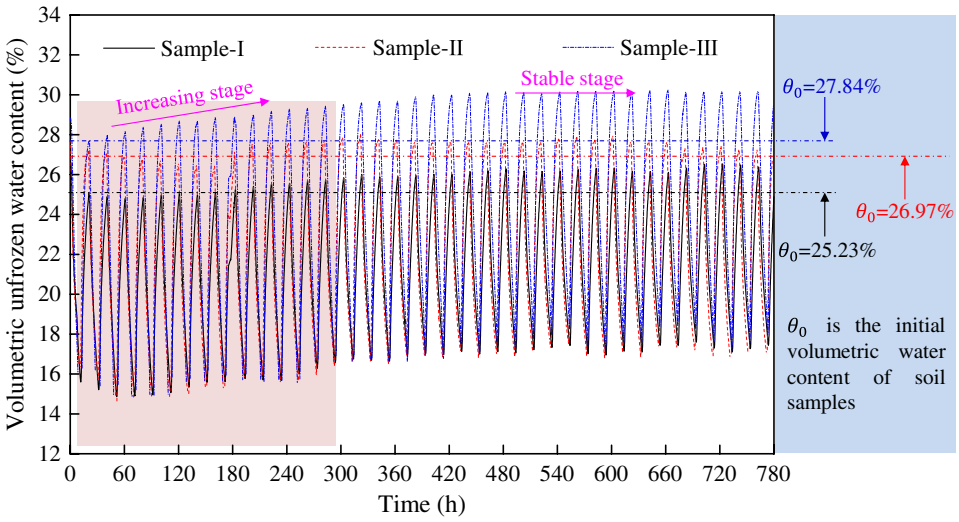

Fig. 5 Volumetric unfrozen water contents versus time for the soil sample nos. I, II, and III

volumetric unfrozen water contents seldom changed with freeze–thaw cycles (Figs. 5 and 6). This might be due to the water migration, seepage, and water distribution during freezing and thawing processes.

Besides, Figs. 5 and 6 also show that the controlled ambient temperatures greatly influenced on the volumetric unfrozen water contents, especially on the residual volumetric unfrozen water contents, which are mainly related to the lowest ambient temperatures. Namely, the residual volumetric unfrozen water contents under the controlled ambient temperature condition 1 (the lowest ambient temperature is − 8.0 °C) are lower than those for the controlled ambient temperature condition 2 (the lowest ambient temperature is − 3.0 °C) (Figs. 4, 5 and 6). Furthermore, under the same ambient temperatures, the initial water contents rarely influence the residual volumetric unfrozen water contents, e.g., for the soil sample nos. I, II, and III (controlled ambient temperature condition 1), the residual volumetric unfrozen water contents varied from 14.9 to 17.2% (Figs. 4 and 5), and for the soil samples nos. IV, V, and VI (controlled ambient temperature condition 2), the residual volumetric unfrozen water contents varied from 18.4 to 20.6% (Figs. 4 and 6).

From the above analyses, it is found that the maximum volumetric unfrozen water contents changed with the freeze–thaw cycles (Figs. 5 and 6). Generally, during the freeze–thaw cycles, there are two factors affecting the distribution of volumetric unfrozen water in the soil samples, namely, water seepage and water migration (Fig. 7). During the freezing processes, liquid water in soil samples can migrate from unfrozen zone to frozen zone under temperature gradients, which would lead into the increase of water contents of frozen zone. Simultaneously, during the freezing and thawing processes, water seepage occurs under the gravity (Fig. 7). Therefore, it is necessary to investigate which

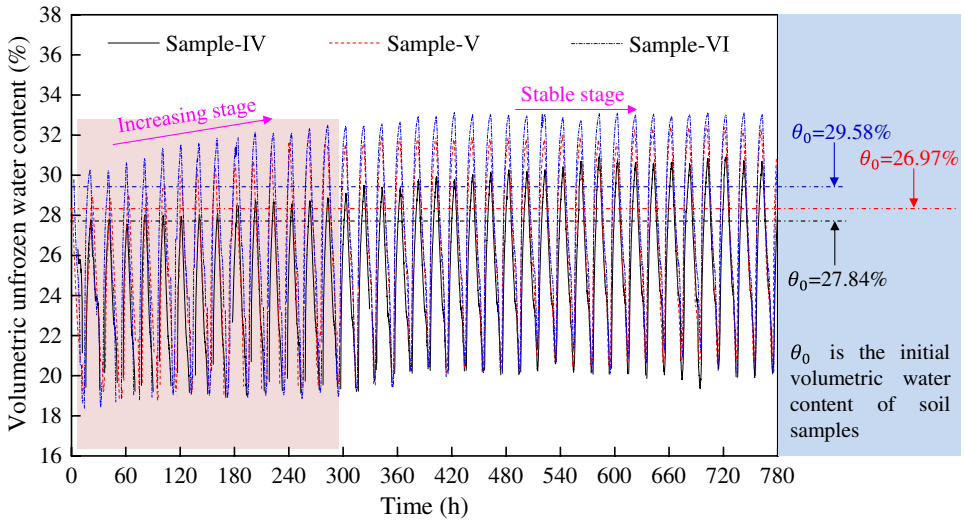

Fig. 6 Volumetric unfrozen water contents versus time for the soil sample nos. IV, V, and VI

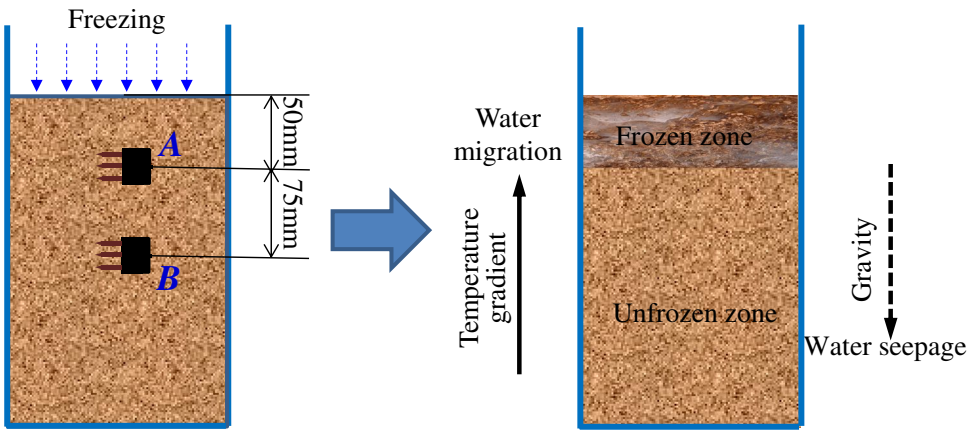

Fig. 7 Water flow in soil during freezing and thawing processes

of the two factors is more important on the redistribution of unfrozen water contents under the freeze–thaw actions.

Figure 8 shows the volumetric unfrozen water contents at different positions of soil sample no. VI during the freeze–thaw cycles, where points A and B are located at the depth of 50 mm and 125 mm from the top of soil samples, respectively (Fig. 7). Figure 8 shows that during the freeze–thaw cycles, the variations of maximum volumetric unfrozen water contents at points A and B can be divided into two stages, while there are different change trends for points A and B during the first fifteen freeze–thaw cycles (Fig. 8). For the point A (depth of 50 mm from the top), the maximum volumetric unfrozen water content decreases, while the reverse trend occurs for the point B (depth of 125 mm from the top) (Fig. 8). Besides, it also presents that in the first fifteen freeze–thaw cycles, the maximum volumetric unfrozen water content at point B is lower than that at point A. Therefore, it could be concluded that the influence of water seepage on volumetric unfrozen water contents during the freezing and thawing processes is larger than that of the water migration during the freezing processes. After the first fifteen freeze–thaw cycles, the maximum volumetric unfrozen water contents for the two points tends to be stable (Fig. 8).

Analysis of deformation behaviors

Figure 9 presents the variation of deformation with time for different soil samples. The figure shows that the deformations rapidly change from the first to the fifteen freeze–thaw cycles, and then slowly change with freeze–thaw cycles (Fig. 9). Moreover, the freeze–thaw cycles significantly influence the deformation of soil samples with different initial dry densities. For the soil samples with low dry densities, i.e., soil sample no. I (ρ_d = 1.45g/cm^3) and soil sample no. II (ρ_d = 1.55g/cm^3), the deformations decrease with

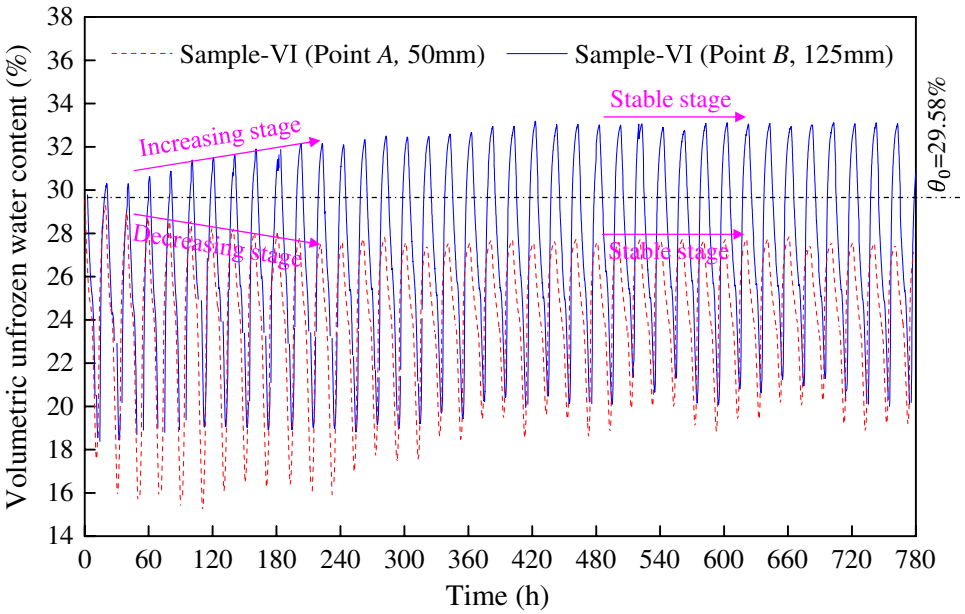

Fig. 8 Volumetric unfrozen water contents at different positions of soil sample no. VI during freeze–thaw cycles

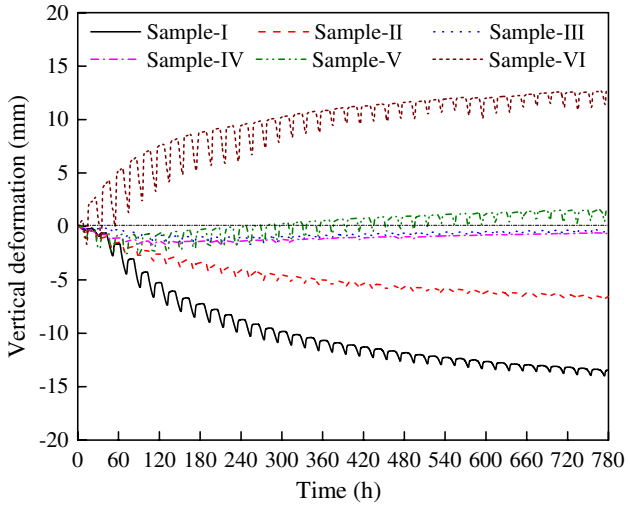

Fig. 9 Variations of deformation with time for different soil samples

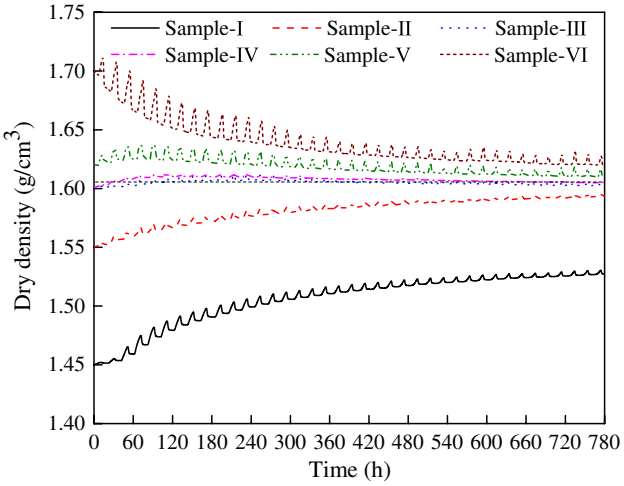

Fig. 10 Variations of dry densities with time for different soil samples

freeze–thaw cycles. It indicates that the volumes compressed and net compactions occur, and after the freeze–thaw cycles, the final net deformation for the soil sample nos. I and II (initial dry density less than 1.60 g/cm^3) are − 13.45 mm and − 6.57 mm (negative values represent compression), respectively (Fig. 9). However, for the soil sample with high dry densities, i.e., soil sample no. VI (ρ_d = 1.70g/cm^3), the deformation increases with freeze–thaw cycles, which means that the volume expands and net heave occurs, the final net deformation for the soil sample no. VI is 12.7 mm (positive values represent heave) (Fig. 9).

Additionally, for the soil sample nos. III and IV (ρ_d = 1.60g/cm^3), and the soil sample no. V (ρ_d = 1.62g/cm^3), the deformations seldom change with freeze–thaw cycles, and the final net deformations of the soil samples nos. III, IV and V are − 0.31, − 0.65 and 1.54, respectively (Fig. 9). It is preliminarily concluded that there is a critical dry density where the soil sample seldom change its volume after freeze–thaw cycles.

It has been found that the dense soils with high densities are expanded (heave), while the soils with low densities are compressed (settlement) after freeze–thaw cycles (Fig. 9). It indicates that there is a critical dry density and critical porosity where the soil samples does not change its volumes, dry densities and porosities. Therefore, it is significant to find the critical dry density and critical porosity of soils, which will give important guidance for the construction, operation, and maintenance of engineering in cold regions.

The dry density of soil samples during the freeze–thaw processes could be obtained as,

$$\rho_d = \frac{4m_s}{\pi d^2(h_0 + \Delta h)} \tag{3}$$

where m_s is the mass of the dry soils; d, h_0, and Δh are the diameter, initial height, and deformation of soil samples, respectively.

Thus, the porosity of soil samples is expressed:

$$n = 1 - \frac{\rho_d}{G_s} \tag{4}$$

where G_s is the density of soil particle.

Figure 10 shows the variations of the dry densities for different soil samples during freeze–thaw cycles, it presents the dry densities decrease for the dense soil sample no. VI (ρ_d = 1.70g/cm^3) and increase for the loose soil sample nos. I (ρ_d = 1.45g/cm^3) and II (ρ_d = 1.55g/cm^3) under the actions of freeze–thaw cycles. Besides, for the soil sample no. V (ρ_d = 1.62g/cm^3), the dry density slightly decreases. However, for the soil sample nos. III and IV (ρ_d = 1.60g/cm^3), the dry densities seldom change during the freeze–thaw cycles (Fig. 10). Therefore, it is concluded that the critical dry density of the silty clay is around 1.60 g/cm^3 during the freeze–thaw cycles.

Considering the opposite influences of freeze–thaw actions on the dense and loose soils, a residual porosity was proposed, which meant that both dense and loose soils would tend to the residual porosity after a certain number of freeze–thaw actions (Viklander 1998). Figure 11 presents the variations of porosities for different soil samples during the freeze–thaw cycles. It shows that, the porosities of the soil sample nos. I and II decrease after the freeze–thaw actions, ranging from 0.46 to 0.43 for soil sample no. I, and ranging from 0.43 to 0.41 for soil sample no. II. While reversed change occurs for the soil sample no. VI, the porosity ranges from 0.37 to 0.40 after the freeze–thaw cycles (Fig. 11). Besides, under the freeze–thaw cycles, the porosities of soil sample nos. III, IV, and V seldom change (Fig. 11). It can

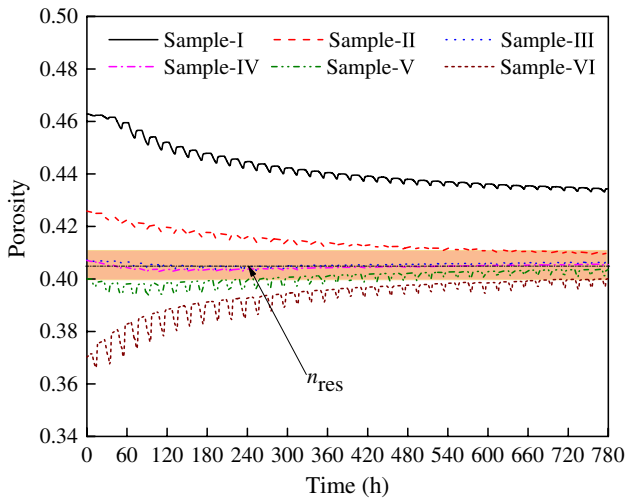

Fig. 11 Variations of porosities with time for different soil samples

be obtained that the residual porosity of the silty clay is ranging from 0.40 to 0.41, although the porosities of soil sample nos. I, II, and VI does not change to the interval of 0.40 to 0.41, which may be due to factors, i.e., number of freeze–thaw cycles.

Conclusions

This paper experimentally investigated the influence of freeze–thaw cycles on the hydro-thermal characteristics and deformation behaviors of a silty clay, and some conclusions are drawn:

(1) The volumetric unfrozen water content, deformation, dry density and porosity of the silty clay rapidly change in the first fifteen freeze–thaw actions, and tend to be stable with freeze–thaw cycles. It indicates that the influences of freeze–thaw cycles on the hydro-thermal characteristics and deformation behaviors of the soil mainly occur in the first freeze–thaw cycles.

(2) The controlled ambient temperatures significantly influence the volumetric unfrozen water contents, and the residual volumetric unfrozen water contents of soils are mainly related to the lowest ambient temperature. Besides, during freeze–thaw cycles, the influence of water seepage on volumetric unfrozen water contents is larger than that of the water migration.

(3) The freeze–thaw cycles have opposite effects on the dense and loose soils, i.e., the dense soils with high densities are expanded (heave), while the soils with low densities are compressed (settlement) after freeze–thaw cycles. Furthermore, for the silty clay, the critical dry density and residual porosity are around 1.60 g/cm^3 and 0.40 ~ 0.41, respectively. Therefore, for the construction of practical engineering in cold regions, it is important to determine the critical dry density of soils and roll to the residual porosity for some civil engineering (e.g., subgrade filling) exposed to drastically freeze–thaw cycles.

Funding This research was supported by the National Natural Science Foundation of China (Grant Nos. 42101136, 42071087), the China Postdoctoral Science Foundation (Grant No. 2021M692697), the State Key Laboratory of Frozen Soil Engineering (Grant No. SKLFSE202007), the Sichuan Science and Technology Program (Grant No. 2021YFQ0021), and the Sichuan Youth Science and Technology Innovation Research Team (Grant No. 2019JDTD0017).

Data availability Not applicable.

Code availability Not applicable.

Declarations

Conflict of interest The authors declare no competing interests.

References

Aldaood A, Bouasker M, Al-Mukhtar M (2016) Effect of water during freeze–thaw cycles on the performance and durability of lime-treated gypseous soil. Cold Reg Sci Technol 123:155–163. https://doi.org/10.1016/j.coldregions.2015.12.008

Chamberlain EJ, Gow AJ (1979) Effect of freezing and thawing on the permeability and structure of soils. Eng Geol 13:73–92. https://doi.org/10.1016/0013-7952(79)90022-X

Cui ZD, He PP, Yang WH (2014) Mechanical properties of a silty clay subjected to freezing–thawing. Cold Reg Sci Technol 98:26–34. https://doi.org/10.1016/j.coldregions.2013.10.009

Eller H, Denoth A (1996) A capacitive soil moisture sensor. J Hydrol 185:1–4. https://doi.org/10.1016/0022-1694(95)03003-4

Hohmann-Porebska M (2002) Microfabric effects in frozen clays in relation to geotechnical parameters. Appl Clay Sci 21:77–87. https://doi.org/10.1016/S0169-1317(01)00094-1

Kalkan E (2009) Effects of silica fume on the geotechnical properties of fine-grained soils exposed to freeze and thaw. Cold Reg Sci Technol 58:130–135. https://doi.org/10.1016/j.coldregions.2009.03.011

Kamei T, Ahmed A, Shibi T (2012) Effect of freeze–thaw cycles on durability and strength of very soft clay soil stabilised with recycled Bassanite. Cold Reg Sci Technol 82:124–129. https://doi.org/10.1016/j.coldregions.2012.05.016

Kozlowski T, Nartowska E (2013) Unfrozen water content in representative bentonites of different origin subjected to cyclic freezing and thawing. Vadose Zone J 12(vzj2012):0057. https://doi.org/10.2136/vzj2012.0057

Lai YM, Wu DY, Zhang MY (2017) Crystallization deformation of a saline soil during freezing and thawing processes. Appl Therm Eng 120:463–547. https://doi.org/10.1016/j.applthermaleng.2017.04.011

Li SY, Lai YM, Pei WS, Zhang SJ, Zhong H (2014) Moisture–temperature changes and freeze–thaw hazards on a canal in seasonally

frozen regions. Nat Hazards 72:287–308. https://doi.org/10.1007/s11069-013-1021-3
Li SY, Zhang MY, Tian YB, Pei WS, Zhong H (2015) Experimental and numerical investigations on frost damage mechanism of a canal in cold regions. Cold Reg Sci Technol 116:1–11. https://doi.org/10.1016/j.coldregions.2015.03.013
Li SY, Niu FJ, Lai YM, Pei WS, Yu WB (2017a) Optimal design of thermal insulation layer of a tunnel in permafrost regions based on coupled heat-water simulation. Appl Therm Eng 110:1264–1273. https://doi.org/10.1016/j.applthermaleng.2016.09.033
Li GY, Ma W, Mu YH, Wang F, Fan SZ, Wu YH (2017b) Effects of freeze-thaw cycle on engineering properties of loess used as road fills in seasonally frozen ground regions, North China. J Mt Sci 14:356–368. https://doi.org/10.1007/s11629-016-4005-4
Liu WB, Yu WB, Yi X, Chen L, Han FL, Hu D (2015) Thermal regime of frozen soil foundation affected by concrete base of transmission line tower on the Tibetan Plateau. Appl Therm Eng 75:950–957. https://doi.org/10.1016/j.applthermaleng.2014.10.041
Liu ZY, Liu JK, Li X, Fang JH (2019a) Experimental study on the volume and strength change of an unsaturated silty clay upon freezing. Cold Reg Sci Technol 157:1–12. https://doi.org/10.1016/j.coldregions.2018.09.008
Liu XQ, Liu JK, Tian YH, Chang D, Hu TF (2019b) Influence of the freeze-thaw effect on the Duncan-Chang model parameter for lean clay. Transp Geotech 21:100273. https://doi.org/10.1016/j.trgeo.2019.100273
Lu JG, Zhang MY, Zhang XY, Pei WS, Bi J (2018) Experimental study on the freezing–thawing deformation of a silty clay. Cold Reg Sci Technol 151:19–27. https://doi.org/10.1016/j.coldregions.2018.01.007
Lu JG, Zhang MY, Pei WS (2019) Hydro-thermal behaviors of the ground under different surfaces in the Qinghai-Tibet Plateau. Cold Reg Sci Technol 161:99–106. https://doi.org/10.1016/j.coldregions.2019.03.002
Lu JG, Wan XS, Yan ZR, Qiu EX, Pirhadi N, Liu JN (2021) Modeling thermal conductivity of soils during a freezing process. Heat Mass Transf 575:976–986. https://doi.org/10.1007/s00231-021-03110-0
Ma W, Mu YH, Zhang JM, Yu WB, Zhou ZW, Chen T (2019) Lateral thermal influences of roadway and railway embankments in permafrost zones along the Qinghai-Tibet Engineering Corridor. Transp Geotech 21:100285. https://doi.org/10.1016/j.trgeo.2019.100285
Moghbel F, Fall M (2016) Response of compost biocover to freeze-thaw cycles: Column experiments. Cold Reg Sci Technol 131:39–45. https://doi.org/10.1016/j.coldregions.2016.09.005
Qi JL, Vermeer PA, Cheng GD (2006) A review of the influence of freeze-thaw cycles on soil geotechnical properties. Permafrost Periglac Process 17:245–252. https://doi.org/10.1002/ppp.559
Qi JL, Ma W, Song CX (2008) Influence of freeze–thaw on engineering properties of a silty soil. Cold Reg Sci Technol 53:397–404. https://doi.org/10.1016/j.coldregions.2007.05.010
Simonsen E, Janoo V, Isacsson U (2002) Resilient properties of unbound roadmaterials during seasonal frost conditions. J Cold Reg Eng 16:28–50. https://doi.org/10.1061/(ASCE)0887-381X(2002)16:1(28)
Tian HH, Wei CF, Lai YM, Chen P (2018) Quantification of water content during freeze-thaw cycles: A Nuclear magnetic resonance based method. Vadose Zone J 17:160124. https://doi.org/10.2136/vzj2016.12.0124
Tian HH, Wei CF, Tan L (2019) Effect of freezing-thawing cycles on the microstructure of soils: A two-dimensional NMR relaxation analysis. Cold Reg Sci Technol 158:106–116. https://doi.org/10.1016/j.coldregions.2018.11.014
Topp GC, Davis JL, Annan AP (1980) Electromagnetic determination of soil water content: measurement in coaxial transmission lines. Water Resour Resour 16:574–582. https://doi.org/10.1029/WR016i003p00574
Viklander P (1998) Permeability and volume changes in till due to cyclic freeze-thaw. Can Geotech J 35:471–477
Viklander P, Eigenbrod D (2000) Stone movements and permeability changes in till caused by freezing and thawing. Cold Reg Sci Technol 31:151–162. https://doi.org/10.1139/t98-015
Wan XS, Hu QJ, Liao M (2017) Salt crystallization in cold sulfate saline soil. Cold Reg Sci Technol 137:36–47. https://doi.org/10.1016/j.coldregions.2017.02.007
Wan XS, Gong FM, Qu MF, Qiu EX, Zhong CM (2019) Experimental study of the salt transfer in a cold sodium sulfate soil. KSCE J Civ Eng 23:1573–1585. https://doi.org/10.1007/s12205-019-0905-5
Wu QB, Niu FJ (2012) Permafrost changes and engineering stability in Qinghai-Xizang Plateau. Chin Sci Bull 58:1079–1094. https://doi.org/10.1007/s11434-012-5587-z
Yao XL, Qi JL, Ma W (2009) Influence of freeze–thaw on the stored free energy in soils. Cold Reg Sci Technol 56:115–119. https://doi.org/10.1016/j.coldregions.2008.11.001
Zhang MY, Pei WS, Lai YM, Niu FJ, Li SY (2017a) Numerical study of the thermal characteristics of a shallow tunnel section with a two-phase closed thermosyphon group in a permafrost region under climate warming. Int J Heat Mass Transf 104:952–963. https://doi.org/10.1016/j.ijheatmasstransfer.2016.09.010
Zhang MY, Pei WS, Li SY, Lu JG, Jin L (2017b) Experimental and numerical analyses of the thermo-mechanical stability of an embankment with shady and sunny slopes in a permafrost region. Appl Therm Eng 127:1478–1487. https://doi.org/10.1016/j.applthermaleng.2017.08.074
Zhang XY, Zhang MY, Lu JG, Pei WS, Yan ZR (2017c) Effect of hydro-thermal behavior on the frost heave of a saturated silty clay under different applied pressures. Appl Therm Eng 117:462–467. https://doi.org/10.1016/j.applthermaleng.2017.02.069
Zhang MY, Lu JG, Lai YM, Zhang XY (2018a) Variation of the thermal conductivity of a silty clay during a freezing-thawing process. Int J Heat Mass Transf 124:1059–1067. https://doi.org/10.1016/j.ijheatmasstransfer.2018.02.118
Zhang MY, Zhang XY, Lai YM, Lu JG, Wang C (2018b) Variations of the temperatures and volumetric unfrozen water contents of fine-grained soils during a freezing–thawing process. Acta Geotech 15:595–601. https://doi.org/10.1007/s11440-018-0720-z
Zhao FT, Chang LJ, Zhang WY (2020) Experimental investigation of dynamic shear modulus and damping ratio of Qinghai-Tibet frozen silt under multi-stage cyclic loading. Cold Reg Sci Technol 170:102938. https://doi.org/10.1016/j.coldregions.2019.102938
Zhang MY, Lu JG, Pei WS, Lai YM, Yan ZR, Wan XS (2021) Laboratory study on the frostproof performance of a novel embankment dam in seasonally frozen regions. J Hydrol. https://doi.org/10.1016/j.jhydrol.2021.126769